

PREDICTIVE CURRENT CONTROLLER WITH MTPA CONTROL STRATEGY – SIMULATION RESULTS

Rafał Piotuch

West Pomeranian University of Technology in Szczecin, Electric Department

Abstract. Electric and hybrid vehicle drive systems are commonly equipped with Permanent Magnet Synchronous Motors, because they offer high efficiency in broad range of speed and torque, and also due to special current development techniques they can work with high speeds. The paper presents simulation results for predictive current controller used in PMSM drive system. The results were obtained for high speed operations with Maximum Torque Per Ampere (MTPA) control strategy, which allows to develop set torque value with the smallest possible currents values. Predictive current controller equations are based on IPMSM mathematical model which considers L_d and L_q inductances changes. Additionally MTPA strategy also considers inductances changes in d - and q -axis.

Keywords: synchronous machine, predictive current controller, MTPA strategy, field analysis

PREDYKCYJNY REGULATOR PRĄDU W STRATEGII MTPA – BADANIA SYMULACYJNE

Streszczenie. Układy napędowe samochodów elektrycznych i hybrydowych są coraz częściej wyposażane w silniki elektryczne z magnesami trwałymi. Napędy te oferują wysoką sprawność w szerokim zakresie prędkości i momentu obrotowego, a poprzez odpowiednie sterowanie zapewniają pracę przy wysokich prędkościach obrotowych. W pracy przedstawiono wyniki badań symulacyjnych predyktoryjnego regulatora prądu dla silnika synchronicznego z magnesami zagnieżdżonymi. Regulator pracuje przy wykorzystaniu strategii sterowania MTPA (ang. Maximum Torque Per Ampere), która zapewnia wypracowanie odpowiedniego momentu przy możliwie najmniejszych wartościach prądów fazowych. Równania predyktoryjnego regulatora prądu zostały oparte o zmodyfikowany model matematyczny silnika synchronicznego z magnesami zagnieżdżonymi uwzględniający zmienność indukcyjności L_d i L_q . Dodatkowo w równaniach opisujących działanie strategii MTPA uwzględniono zmienność indukcyjności w funkcji prądu.

Słowa kluczowe: maszyna synchroniczna, predyktoryjny regulator prądu, strategia MTPA, analiza polowa

Introduction

PM excited machines are receiving increased attention in drive systems applications instead of induction motor because of high power density, efficiency, high torque-inertia ratio and wide speed operation capabilities which makes it particularly suitable for all automotive applications where weight and geometry dimensions are very important. In particular, an IPMSM with permanent magnets buried inside steel rotor core perform mechanically robust rotor structure which is suitable for high-speed operation applications. Very important aspect of electric vehicle drive system is an energy efficient torque development, which can be achieved with MTPA control strategy and proper current controller or other adaptive or heuristics methods [4]. Additionally Field-Weakening (FW) strategy increases Constant Power Speed Range (CPSR). Wide speed range with constant power is required especially for the traction drive applications. CPSR depends on inductances and magnet flux values and power supply constraints. Unfortunately magnetic saturation may occur under different speed and load conditions resulting in the variation of the d - and q -axis inductances [1, 5, 6]. The variation of inductances is especially strong in IPMSMs and it is important to note that the performance of the drive is rather sensitive to machine parameters, especially for high torque regions.

In this paper there will be described the proposed algorithm starting from the mathematical model used to calculate the d - and q -axis reference currents in the constant torque region. In the constant torque region the requirements are maximum efficiency of the drive or a good dynamic performance of the drive. The paper present equation set and achieved results.

1. IPMSM modeling

Fig. 1 shows a four pole IPM motor, which was used in the simulations. The following equations that describe work of a PM Synchronous motor are basic voltage and flux-current equations described in synchronous dq reference frame under several assumptions [8]:

$$U_d = R_s I_d + \frac{d\Psi_d}{dt} - p_b \Omega_m \Psi_q \quad (1)$$

$$U_q = R I_q + \frac{d\Psi_q}{dt} + p_b \Omega_m \Psi_d \quad (2)$$

$$\Psi_d = L_d I_d + \Psi_{PM} \quad (3)$$

$$\Psi_q = L_q I_q \quad (4)$$

Torque developed by a PM excited motor can be expressed as:

$$T_{em} = \frac{3}{2} \cdot p_b \cdot [\Psi_{PM} \cdot I_{sq} + (L_d - L_q) \cdot I_{sd} \cdot I_{sq}] \quad (5)$$

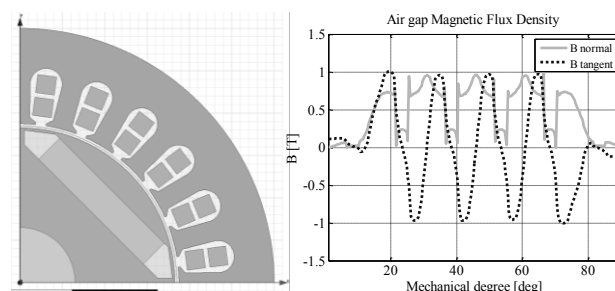


Fig. 1. IPMSM cross-section and magnetic flux distribution along pole

Table 1. Main parameters of the machine

Parameter	Value
Magnet type	XG196/96 (B=0.96T, Hc=-690kA)
Outer stator diameter	120 mm
Active machine length	65 mm
Rotor outer diameter	73 mm
Magnet length	35 mm
Magnet width	7 mm
Slot opening width	3 mm
Tooth width	7.3 mm
Slot height	13.5 mm
Air gap length	1 mm

2. IPMSM torque development

Torque developed by IPM motor can be divided into PM generated and reluctance torque components (Fig. 2).

The first term is PM generated torque, and the second term is reluctance torque which is proportional to the difference in stator inductances, L_d and L_q . In the analyzed IPMSM, L_q is higher than L_d (due to the lower q -axis path reluctance), because the magnetic flux flowing along the d -axis has to cross through the magnet cavities in addition to the rotor air gap, while the magnetic flux of the q -axis crosses only the air gap. The d -axis is also basically magnetized with PM [2].

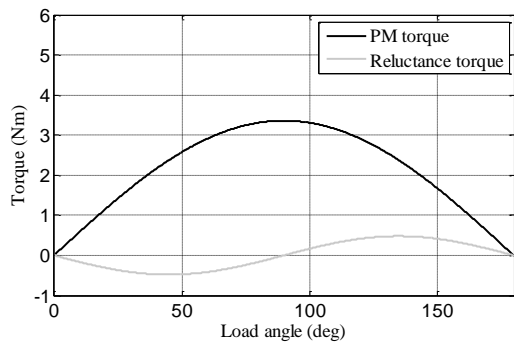


Fig. 2. Example of torque curves

Equation (5) may also consider L_d and L_q changes:

$$T_{em} = \frac{3}{2} \cdot p_b \cdot \left[\Psi_{PM} \cdot I_q + (L_d(I_d) - L_q(I_q)) \cdot I_d \cdot I_q \right] \quad (6)$$

Properly controlled currents in motor windings give a possibility to control synchronous machine in a similar manner to a separately excited DC machine, where flux and torque (with constant flux) can be controlled separately [1, 4].

3. MTPA control strategy

Basic FOC (Field Oriented Control) structure consist of four PI controllers (Fig. 3).

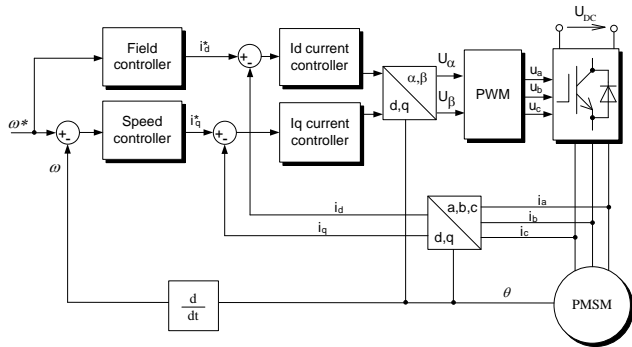
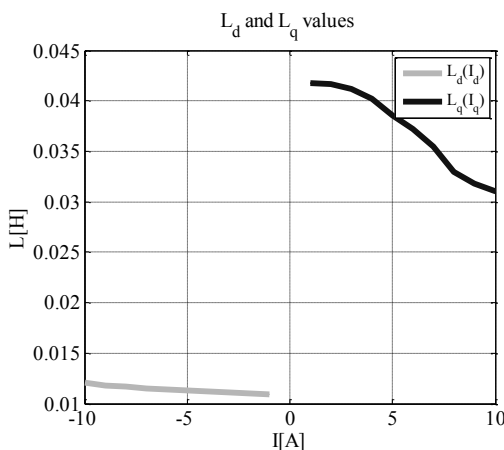


Fig. 3. Basic FOC control scheme

The aim of a current controllers is to develop proper current values in d - and q -axis according to a selected control strategy. It keeps such torque value that causes a 0 speed error value. Basically there are main four controller strategies [2]:

- 1) CTA (Constant Torque Angle),
- 2) UPF (Unity Power Factor),
- 3) CSF (Constant Stator Flux),
- 4) MTPA (Maximum Torque Per Ampere).

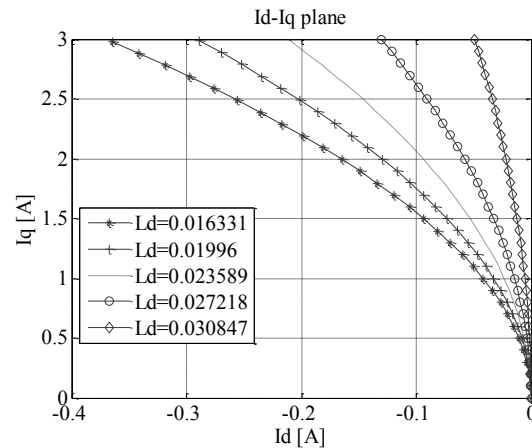
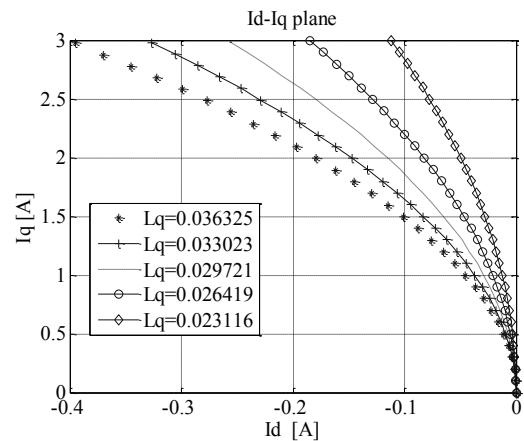
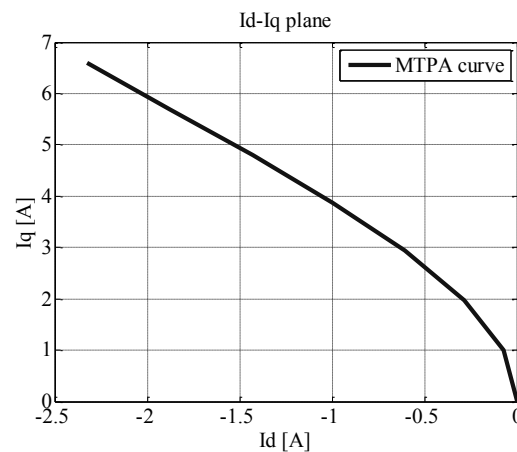
As shown in Fig. 2 the main torque component is developed with q -axis current. With MTPA control strategy application it is also possible to take advantage of reluctance torque according to (5, 6).

Fig. 4. L_d and L_q inductances based on FEM simulation

This way the smallest possible phase currents develop set torque value. The copper losses are minimized, and under assumption that core losses are negligible (which for low speeds and torques is generally true) the maximum efficiency of the IPMSM can be obtained.

It is needed to estimate and use L_d , L_q inductances values for different stator currents [7] – according to equation (6). Calculated inductance values for different currents are shown in the Fig. 4.

The $i_d - i_q$ planes with MTPA curve for different L_d and L_q values are presented in Fig. 5 and 6. The $i_d - i_q$ plane with MTPA considering changing values of L_d and L_q (according to Fig. 4) is shown in Fig. 7.

Fig. 5. MTPA curve for different L_d inductance valuesFig. 6. MTPA curve for different L_q inductance valuesFig. 7. MTPA curve for estimated L_d and L_q inductances values

The problem arises when the flux from magnets gives high electro-motive force, in the high speed regions, which results in exceeded supply voltage. Using d -axis negative current main flux is decreased and thus it is possible to stay in the voltage limit. This method is called field weakening method.

The control strategy meets several limitations:

$$U_d^2 + U_q^2 < U_N^2 \quad (7)$$

$$I_d^2 + I_q^2 < I_N^2 \quad (8)$$

Evaluating voltages and current constraints it is possible to identify two main regions [4]:

- 1) Constant Torque Region,
- 2) Constant Power Region.

The second one will be a subject of the next author paper.

4. Predictive current controller

The paper is focused on nonlinear current controllers. Each control system, which uses information of an object in order to develop optimal control signals can be included to the predictive controllers group. Fig. 8 presents the idea of a predictive current controller work.

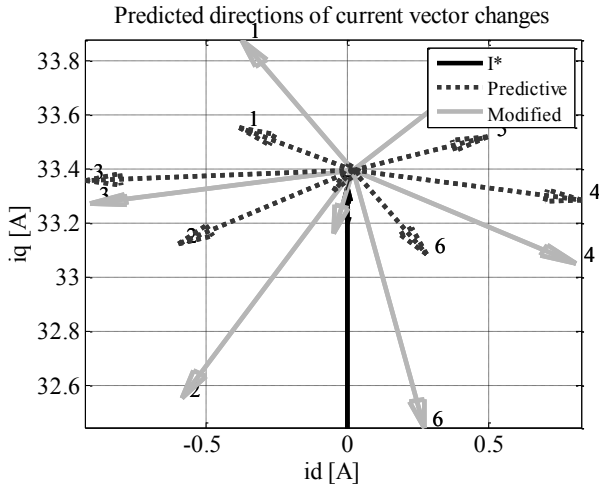


Fig. 8. Predictive algorithm work scheme

Considering (1-4) equations it is possible to define following equations for stator current derivatives:

$$\begin{bmatrix} \dot{i}_d(t) \\ \dot{i}_q(t) \end{bmatrix} = \begin{bmatrix} -\frac{R}{L_d} & \omega(t) \\ -\omega(t) & -\frac{R}{L_q} \end{bmatrix} \begin{bmatrix} i_d(t) \\ i_q(t) \end{bmatrix} + \begin{bmatrix} \frac{1}{L_d} & 0 & 0 \\ 0 & \frac{1}{L_q} & -\frac{\omega(t)}{L_d} \end{bmatrix} \begin{bmatrix} u_d(t) \\ u_q(t) \\ \Psi_{PM} \end{bmatrix} \quad (9)$$

where i_d, i_q – stator currents, u_d, u_q – stator voltages, R – stator phase resistance, L_d, L_q – d - and q -axis inductances, Ψ_{PM} – permanent magnet flux in the air gap. Considering very small time step – smaller than electromechanical and electrical time constant it is possible to assume that the position and speed change is negligible. In this case equations (1, 2) can be written as:

$$\begin{bmatrix} i_d(k+1) \\ i_q(k+1) \end{bmatrix} = \begin{bmatrix} 1 - \frac{R \cdot T}{L_d} & T \cdot \omega(k) \\ -T \cdot \omega(k) & 1 - \frac{R \cdot T}{L_q} \end{bmatrix} \begin{bmatrix} i_d(k) \\ i_q(k) \end{bmatrix} + \begin{bmatrix} \frac{T}{L_d} & 0 \\ 0 & \frac{T}{L_q} \end{bmatrix} \begin{bmatrix} v_d(k) \\ v_q(k) \end{bmatrix} + \begin{bmatrix} 0 \\ -\frac{T \cdot \omega(k)}{L_d} \cdot \Psi_{PM} \end{bmatrix} \quad (10)$$

d and q voltages may be presented as follows

$$\begin{bmatrix} v_d(k) \\ v_q(k) \end{bmatrix} = \mathbf{M}(k) \cdot \mathbf{D} \cdot \mathbf{u}(k) \quad (11)$$

$$\mathbf{u}(k) = \begin{bmatrix} u_a(k) \\ u_b(k) \\ u_c(k) \end{bmatrix} \quad (12)$$

$$\mathbf{D} = U_{DC} \cdot \frac{2}{3} \cdot \begin{bmatrix} 1 & -\frac{1}{2} & -\frac{1}{2} \\ 0 & \frac{\sqrt{3}}{2} & -\frac{\sqrt{3}}{2} \end{bmatrix} \quad (13)$$

$$\mathbf{M}(k) = \begin{bmatrix} \cos \theta(k) & \sin \theta(k) \\ -\sin \theta(k) & \cos \theta(k) \end{bmatrix} \quad (14)$$

Finally, the equations that represent future current component vector values, that are developed for the selected voltage vector may be expressed as:

$$\mathbf{X}_i(k+1) = \mathbf{F}(k) \cdot \mathbf{X}(k) + \mathbf{G} \cdot \mathbf{M}(k) \cdot \mathbf{D} \cdot \mathbf{u}_i(k) + \mathbf{H}(k) \quad (15)$$

where:

$$\mathbf{X}(k) = \begin{bmatrix} i_d(k) & i_q(k) \end{bmatrix}^T \quad (16)$$

$$\mathbf{F}(k) = \begin{bmatrix} 1 - \frac{R \cdot T}{L_d} & T \cdot \omega(k) \\ -T \cdot \omega(k) & 1 - \frac{R \cdot T}{L_q} \end{bmatrix} \quad (17)$$

$$\mathbf{G}(k) = \begin{bmatrix} \frac{T}{L_d} & 0 \\ 0 & \frac{T}{L_q} \end{bmatrix} \quad (18)$$

$$\mathbf{H}(k) = \begin{bmatrix} 0 \\ \frac{T \cdot \omega(k)}{L_d} \cdot \Psi_{PM} \end{bmatrix} \quad (19)$$

$\mathbf{u}_i(k)$ is a input voltage vector for all seven inverter key configurations, U_{DC} is a DC bus voltage and T is sample time. Such prediction is realized according to rules of linear extrapolation, that could be based on only one sample [3, 4]. Details are presented in [2-4].

At start of a calculation period, the current and the voltage measurements are done in order to evaluate \mathbf{F} , \mathbf{M} and \mathbf{H} matrices. The future values of current vector are evaluated for each inverter key configuration. From this calculation it is possible to evaluate current change vector for each inverter key configuration (Fig. 8). In the classic predictive current control structure the chosen key configuration is the one that fulfils the control quality indicator. Most popular criteria is the angle between the set current vector and the future current vector or the distance between ends of set and future current vectors. The chosen aim function is expressed as:

$$\min(|\mathbf{X}_i(k+1) - \mathbf{X}^*(k)|) \quad (20)$$

On the basis of predicted current vectors three inverter key configurations (two active and one non-active) which cause current to achieve set value have to be chosen. Two non-active voltage vectors give the same current values but using the proper one it is possible to minimize number of inverter key switchings. Additionally on the basis of simple mathematical rules the times of application for each key configuration is calculated [2, 4]. Nonlinear current controller acts in this way as a voltage space vector modulator. Linear predictive controllers also use equations presented in this paragraph but take advantage of a Pulse Width

Modulator that transforms voltages in two-phase stationary coordinate system to apply proper inverter key configurations.

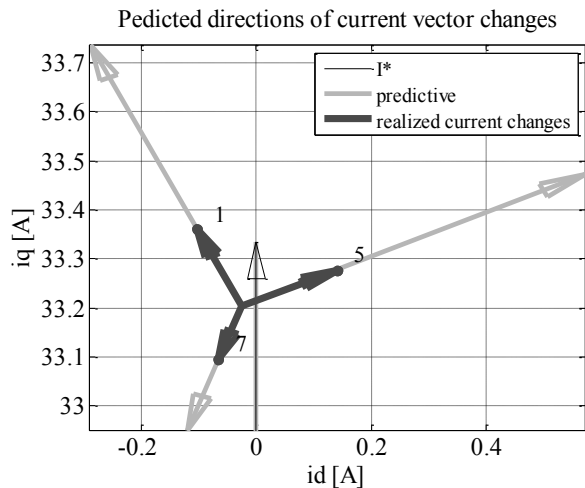


Fig. 9. Realized current vectors (without MTPA)

5. Results

Fig. 10-12 show the results obtained in the Matlab/Simulink environment for the typical work regime – sudden q -axis change (without speed loop) and work of a current controller in static states.

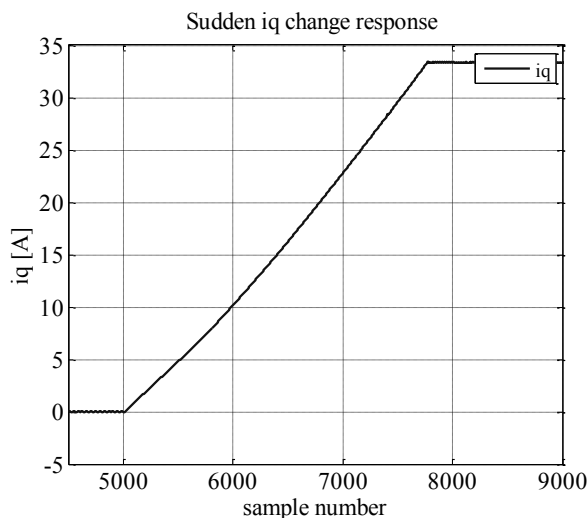


Fig. 10. i_q current dynamics (without MTPA)

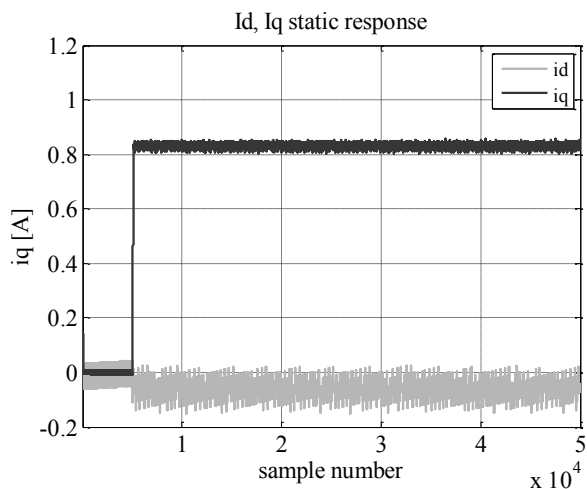


Fig. 11. i_d , i_q statics (with MTPA)

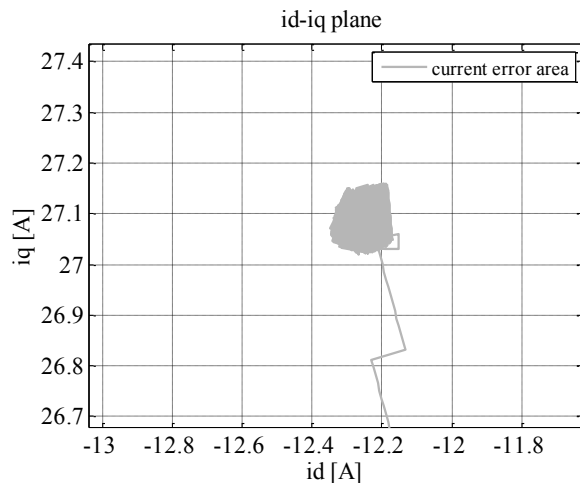


Fig. 12. Current vector error area (with MTPA)

6. Summary

Presented modified predictive current controller with MTPA control strategy and L_d , L_q changes consideration shows very good characteristics in comparison with common current controllers [2-4]. It shows excellent static characteristics and very good dynamic performance. The MTPA strategy with modified predictive current controller performs high dynamic, high efficiency and high torque capabilities which seems to fulfil the requirements for an electric vehicle drive system. A disadvantage of the proposed algorithm is number of calculations which demands powerful DSP to execute calculations in proper time. The current controller may be applied in F28335 Delfino Digital Signal Processor from T.I. thanks to its powerful calculation capabilities and many external interfaces. Not only prediction but also mathematical transformations needed for time recalculation cause high loadings for processor [2, 3].

Bibliography

- [1] Gratkowski S., Pałka R.: Komputerowo wspomagana analiza i projektowanie urządzeń i układów elektromagnetycznych, Wydawnictwo Uczelniane Politechniki Szczecińskiej, Szczecin, 2001.
- [2] Morel F.: Commandes directes appliquées à une machine synchrone à aimants permanents alimentée par un onduleur triphasé à deux niveaux ou par un convertisseur matriciel triphasé, PhD Thesis, France, 2007.
- [3] Morel F., Xuefang L.-S., Rétif J.-M., Allard B.: A predictive current control applied to a permanent magnet synchronous machine, comparison with a classical direct torque control, ScienceDirect, 2008, France.
- [4] Paplicki P., Wardach M., Bonisławski M., Pałka R.: Simulation and experimental results of hybrid electric machine with a novel flux control strategy, Archives of Electrical Engineering, Vol. 64, Iss. 1, 2015, 37-51.
- [5] Piotuch R.: Selected predictive current controllers in PMSM drive systems, post-conference materials, WD 2011, Zielona Góra.
- [6] Piotuch R.: Wyznaczanie indukcyjności z uwzględnieniem nasycenia obwodu magnetycznego maszyn synchronicznych z magnesami zagnieżdżonymi, IAPGOŚ 2/2013, 41-44.
- [7] Rahman M., Zhou P.: Determination of saturated parameters of pm motors using loading magnetic fields, IEEE, Transactions on Magnetics, Vol. 27, No. 5, 1991.
- [8] Tunia H., Kaźmierkowski M.: Podstawy automatyki napędu elektrycznego, PWN, Warszawa, 1983.

M.A. Rafał Piotuch
e-mail: rpiotuch@zut.edu.pl

Rafał Piotuch is an assistant and a Ph.D. student at West Pomeranian University of Technology in Szczecin at the Electric Department. Under prof. Ryszard Pałka supervision he carries out researches on current controllers for permanent magnet excited synchronous machines.



otrzymano/received: 15.10.2013

przyjęto do druku/accepted: 28.04.2015